Oligocene clockwise rotations along the eastern Pamir: Tectonic and paleogeographic implications

Roderic Bosboom, Guillaume Dupont-Nivet, Wentao Huang, Wei Yang, Zhaojie Guo

AGU PUBLICATIONS

Tectonics

RESEARCH ARTICLE

10.1002/2013TC003388

Key Points:

- Paleomagnetic study reveals Oligocene clockwise rotation along eastern Pamir
- Until Miocene Pamir developed symmetrically by radial thrusting
- From Miocene asysmsmetric deformation with transfer faulting along eastern Pamir

Correspondence to:
R. Bosboom,
R.E.Bosboom@uu.nl

Citation:
Bosboom, R., G. Dupont-Nivet, W. Huang, W. Yang, and Z. J. Guo (2014), Oligocene clockwise rotations along the eastern Pamir: Tectonic and paleogeographic implications, *Tectonics*, *33*, 53–66, doi:10.1002/2013TC003388.

Received 6 JUN 2013
Accepted 30 DEC 2013
Accepted article online 5 JAN 2014
Published online 15 FEB 2014

Oligocene clockwise rotations along the eastern Pamir: Tectonic and paleogeographic implications

Roderic Bosboom[1], Guillaume Dupont-Nivet[1,2,3], Wentao Huang[1,2], Wei Yang[2,3], and ZhaoJie Guo[2]

[1]Paleomagnetic Laboratory Fort Hoofddijk, Faculty of Geosciences, Utrecht University, Utrecht, Netherlands, [2]Key Laboratory of Orogenic Belts and Crustal Evolution, Ministry of Education, Peking University, Beijing, China, [3]Géosciences Rennes, UMR-CNRS 6118, Université de Rennes1, Rennes Cedex, France

Abstract Despite the importance of the Pamir range in controlling Asian paleoenvironments and land-sea paleogeography, its tectonic evolution remains poorly constrained in time and space, hindering its potential for understanding deep to surface processes. We provide here new constraints on vertical-axis tectonic rotations from the southwest Tarim Basin along the eastern flank of the Pamir arcuate range based on paleomagnetic results. Two well-dated Eocene to Oligocene sections, previously analyzed using biostratigraphy and magnetostratigraphy, yield consistently clockwise rotations of 21.6 ± 4.2° in 41 to 36 Ma strata then 17.1 ± 6.5° in 33 to 28 Ma strata at the Aertashi section and 14.2 ± 11.5° in 41 to 40 Ma strata at the Kezi section. Combined with a regional review of existing paleomagnetic studies, these results indicate that most of the clockwise rotations along the eastern Pamir occurred during Oligocene times and did not extend systematically and regionally into the Tarim Basin. In contrast, on the western flank of the Pamir tectonic rotations in Cretaceous to Neogene strata are regionally extensive and systematically counterclockwise throughout the Afghan-Tajik Basin. This timing and pattern of rotations is consistent with paleogeographic reconstructions of the regional sea retreat out of Central Asia and supports a two-stage kinematic model: (1) symmetric rotations of either flanks of the Pamir arcuate range until Oligocene times followed by (2) continued rotations on its western flank associated with radial thrusting and, along the eastern flank, no further rotations due to decoupled transfer slip starting in the Early Miocene.

1. Introduction

The arcuate Pamir range (Figure 1) formed during the northward indentation of India into Asia, constituting a prominent tectonic feature and a major paleogeographical divide with important implications on Asian paleoclimate evolution [*Bershaw et al.*, 2012; *Burtman and Molnar*, 1993]. It closed the Tarim Basin to the east from the Afghan-Tajik and Ferghana Basins to the west and partly forced the retreat of an epicontinental sea that formerly extended across Eurasia [*Bosboom et al.*, 2014; *Bosboom et al.*, 2011; *Bosboom*, 2013]. Lithospheric structures below the Pamir inferred from teleseismic and tomographic studies [*Negredo et al.*, 2007; *Sippl et al.*, 2013] suggest a complex history of slab break off, continental subduction inversion, and roll back [e.g., *Sobel et al.*, 2013]. Despite the importance of this range and its potential for understanding deep to surface processes, its tectonic evolution remains poorly constrained in time and space. The general consensus is that the Pamir indented northward ~300 km into the Eurasian continent [e.g., *Burtman and Molnar*, 1993; *Cowgill*, 2010], starting in Early Eocene times as a relatively straight east-west range aligned with the West Kunlun Shan and ending as the highly curved concave southward range observed today. The acquisition of this peculiar geometry has been proposed to be related either to oroclinal bending or radial thrusting associated with regionally extensive vertical-axis rotations [*Bazhenov and Burtman*, 1986; *Bazhenov et al.*, 1994; *Robinson et al.*, 2004; *Strecker et al.*, 1995] or to transfer faulting induced by opposite shear along the eastern (sinistral) and western (dextral) margins of the Pamir with limited to no vertical-axis rotations [*Burtman and Molnar*, 1993; *Searle*, 1996]. Paleomagnetism provides an opportunity to differentiate between these proposed kinematic models by its ability to quantify and date vertical-axis rotations of crustal fragments with respect to a stable continent [*Butler*, 1992]. Paleomagnetic studies in the Afghan-Tajik Basin on the west side of the Pamir have revealed regionally consistent counterclockwise vertical-axis rotations [*Bazhenov and Mikolaichuck*, 2002; *Bazhenov et al.*, 1994; *Burtman*, 2000; *Pozzi and Feinberg*, 1991; *Thomas et al.*, 1993, 1994]. However, along its eastern flank in the Tarim Basin, West Kunlun Shan, Altyn Tagh, and Tian Shan various rotation studies show large discrepancies in both sense and magnitude of rotation [e.g., *Chen et al.*, 1992; *Gilder et al.*, 1996; *Li et al.*, 2013;

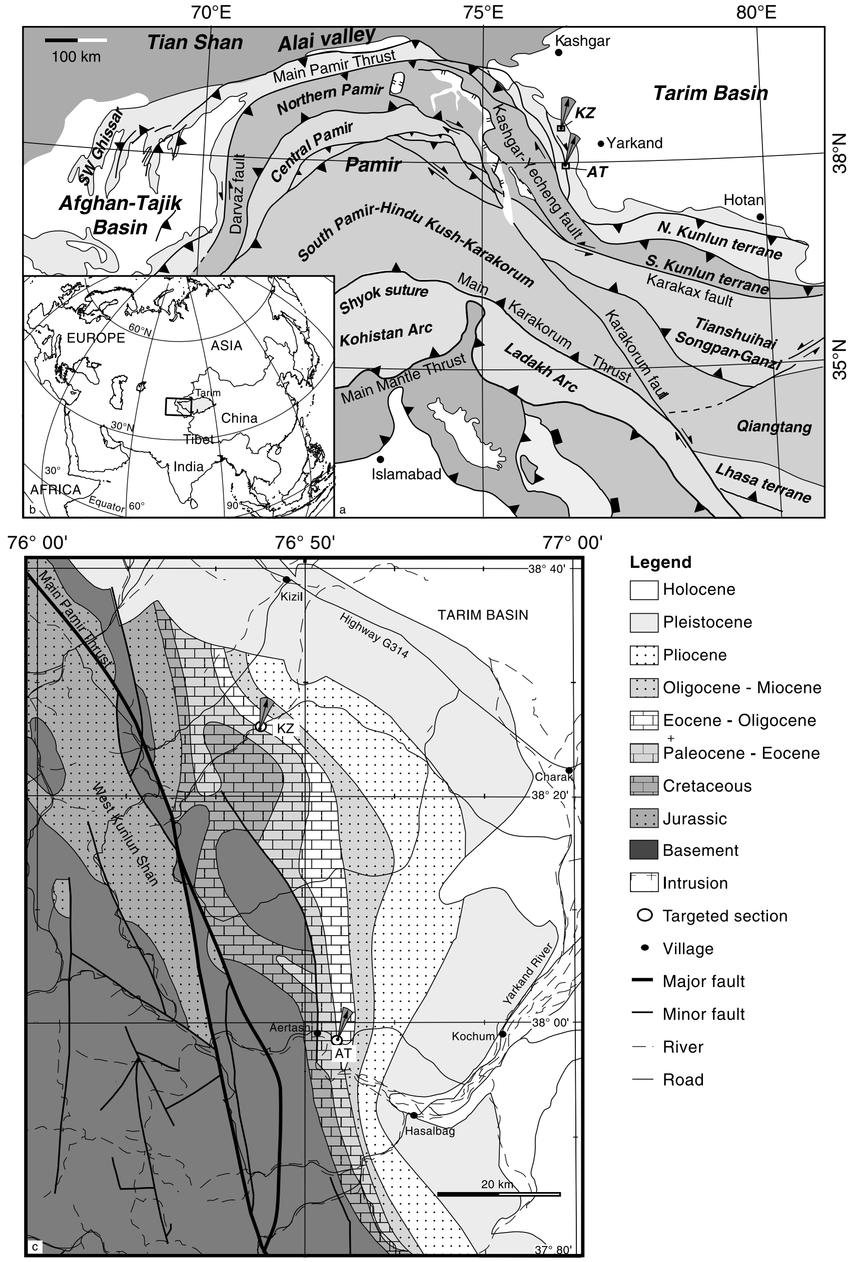

Figure 1. Simplified tectonic map of the Pamir collision zone (modified from *Cowgill* [2010]) showing the calculated rotations and their uncertainties with respect to the Eurasian apparent polar wander path (APWP) at the studied sections of Aertashi (AT) and Kezi (KZ) along the (a) eastern Pamir. (b) The inset shows the regional location of the Tarim Basin (present-day coastal outline obtained from GPlates 0.9.7.1). (c) The detailed geological map of the field area shows the lithostratigraphic units, tectonic features, and locations of the Aertashi (AT) and Kezi (KZ) sections along the eastern margin of the Pamir (modified from the 1:500.000 scale map of the *Bureau of Geology and Mineral Resources of Xinjiang Uygur Autonomous Region* [1993]).

Rumelhart et al., 1999; *Wei et al.*, 2013; *Yin et al.*, 2000], hindering understanding of the kinematics underlying the tectonic evolution of the Pamir.

Here we provide new constraints on the vertical-axis tectonic rotation along the eastern flank of the Pamir (Figure 1), based on paleomagnetic results from two well-dated Eocene to Oligocene sections previously analyzed using bio- and magnetostratigraphy [*Bosboom et al.*, 2013]. We combine our results with a regional review of existing paleomagnetic results to constrain the timing, the sense, the magnitude, and the regional distribution of tectonic deformation and ultimately evaluate the tectonic and paleogeographic evolution of the Pamir.

2. Geological Setting

The Tarim Basin is a relatively undeformed crustal block within the Indo-Asia collision system [*Yin and Harrison*, 2000]. Thrusting and exhumation around the Pamir range is expressed by the Main Pamir Thrust bounding the Alai Valley to the north, the dextral Kashgar-Yecheng transfer system (KYTS) bounding the Tarim Basin on the eastern flank, and the sinistral Darvaz-Karakul strike-slip fault bounding the Afghan-Tajik Basin on the western flank (Figure 1). According to sedimentologic [*Burtman*, 2000; *Yin et al*., 2002], stable isotope and provenance [*Bershaw et al*., 2012], thermochronologic [*Amidon and Hynek*, 2010; *Sobel and Dumitru*, 1997], paleomagnetic [*Thomas et al*., 1994; *Yin et al*., 2002], and backstripping [*Yang and Liu*, 2002] data, these bounding structures are generally thought to have been active mostly into Miocene times with sparse evidence for earlier Eocene initiation.

The sedimentary infill on top of the crustal basement is primarily composed of Paleozoic and Mesozoic clastic sediments, recording the successive distal accretion of continental terranes along the southern margin of Asia from the Late Triassic until the Eocene Indo-Asia collision at ~50 Ma [*Hendrix et al*., 1992; *Jia et al*., 2004; *Robinson et al*., 2003; *Tian et al*., 1989; *van Hinsbergen et al*., 2012; *Yin and Harrison*, 2000]. Distal marginal overthrusting and tectonic loading of the paleo-Tian Shan in the north and the paleo-Pamir-Kunlun orogenic system in the south by the Cenozoic northward movement of India into Eurasia probably initiated two major distal foreland basins, the Kuche depression along the southern margin of the Tian Shan and the southwest depression along the eastern Pamir with its depocenter near Yarkand (Figure 1) [*Burtman and Molnar*, 1993; *Cowgill*, 2010; *Jia et al*., 1997; *Yang and Liu*, 2002; *Yin and Harrison*, 2000]. The progressive and long-term retreat of a shallow sea covering most of the Tarim Basin in the Early Eocene [*Burtman*, 2000; *Burtman et al*., 1996; *Lan and Wei*, 1995; *Tang et al*., 1989] has been related to distal tectonic deformation [e.g., *Bosboom et al*., 2013; *Wei et al*., 2013]. The sea retreated out of the paleodepocenter in the southwest depression in the middle Eocene [*Bosboom et al*., 2011; *Bosboom et al*., 2013] and out of the westernmost Tarim Basin in the Late Eocene [*Bosboom*, 2013]. Thereafter, continental deposition was predominant with relatively distal environments and remnant brackish-marine conditions up into the Oligocene [*Ye et al*., 1996; *Gao et al*., 2000; *Graham et al*., 2005; *Jia et al*., 2004; *Kent-Corson et al*., 2009; *Ritts et al*., 2008; *Zheng et al*., 1999], followed by the Early Miocene initiation of rapid accumulation of coarse-grained clastics in proximal alluvial environments throughout the region [e.g., *Bershaw et al*., 2012; *Charreau et al*., 2005; *Heermance et al*., 2007; *Huang et al*., 2006; *Jia et al*., 2004; *Sobel and Dumitru*, 1997; *Sobel et al*., 2006; *Thomas et al*., 1993, 1994].

The studied sedimentary sections are located along the eastern Pamir (Figure 1) within the western margin of the Tarim Basin, separated from the Pamir by the dextral Kashgar-Yecheng transfer system (KYTS) [*Cowgill*, 2010; *Sobel et al*., 2011]. According to local structural work of *Yin et al*. [2002], the structural style of the studied area is apparently dominated by recent thrusting and dextral slip associated to the Kashgar-Yecheng transfer system (KYTS) and younger deformation.

3. Paleomagnetic Analyses

In order to quantify vertical-axis rotations, we present here the directional analysis of magnetostratigraphic results previously acquired from marine and continental sediments in the southwest Tarim Basin at the Aertashi (37°58′N, 76°33′E) and Kezi (38°26′N, 76°24′E) sections (Figure 1) [*Bosboom et al*., 2013]. *Bosboom et al.* [2013] showed using rock and thermomagnetic analyses that the marine sediments of the Kashi Group at both sections all yielded normal polarity in the present-day field direction before bedding correction. This led *Bosboom et al.* [2013] to conclude that marine strata have been fully remagnetized and are unreliable for any paleomagnetic analyses. These marine sediments are thus unsuitable to infer vertical-axis rotations, although they have been included in some previous studies [e.g., *Chen et al*., 1992; *Huang et al*., 2009; *Rumelhart*, 2000; *Li et al*., 2013]. In contrast, the overlying continental sequence of the Wuqia Group yielded remanent magnetizations of primary origin allowing reliable correlation to the geological timescale [*Gradstein et al*., 2012]. The sampled interval within the Kezilouyi Formation (Figure 2) was constrained in age from the base of C18r to C9n (~41–27 Ma) [*Bosboom et al*., 2013]. A ~3.5 Myr hiatus including the Eocene-Oligocene transition separates the Aertashi section into a lower part (base C18r–C16n.2n; ~41–36 Ma) and an upper part (base C12r–C9n; ~33–27 Ma). At the Kezi section only the very base of the Kezilouyi Formation has been sampled (C18r; ~41–40 Ma). Accordingly, here we use the paleomagnetic results of that continental sequence for the evaluation of the vertical-axis rotations. The ~41 to ~27 Ma deposits are characterized by red siltstones to medium sandstones with cross stratifications and incised channel fills

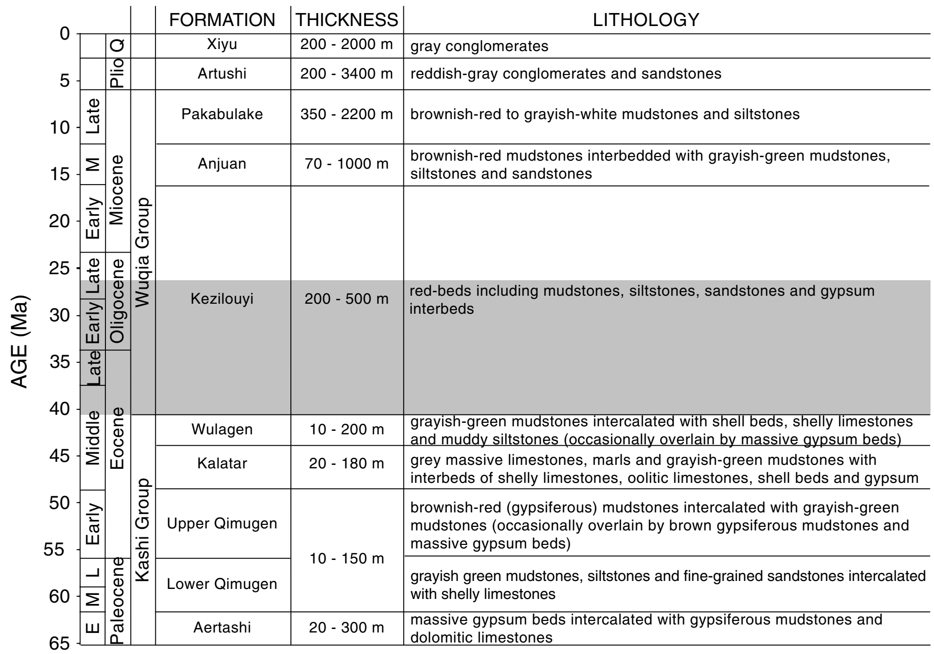

Figure 2. Generalized regional Cenozoic lithostratigraphy of the southwest Tarim Basin. The lithostratigraphy and corresponding thicknesses are summarized from *Jia et al.* [2004], *Mao and Norris* [1988], and *Tang et al.* [1989], whereas the preliminary age estimates are based upon calcareous nanofossils [*Zhong*, 1992], bivalves [*Lan and Wei*, 1995], ostracods [*Yang et al.*, 1995], dinoflagellate cysts [*Mao and Norris*, 1988], benthic foraminifera [*Hao and Zeng*, 1984], and our previous integrated biomagnetostratigraphic study [*Bosboom et al.*, 2013]. The shaded area shows the age range of the continental sediments analyzed in this study.

interbedded by (laminated, gypsiferous) mudstones and are interpreted as representing dominantly alluvial floodplain deposits with occasional (brackish) lacustrine intervals. Accumulation rates are relatively low and range from 5.6 to 23.2 cm/kyr [*Bosboom et al.*, 2013]. The sampled strata are eastward from the eastern Pamir bounding faults and are essentially undisturbed with homoclinal ~15° northeastward dip at Kezi and ~40–65° eastward dip at Aertashi, in line with the trend of regional structures along the eastern Pamir.

Previous paleomagnetic analyses have been carried out in the shielded Paleomagnetic Laboratory "Fort Hoofddijk" of the Faculty of Geosciences at the Utrecht University [*Bosboom et al.*, 2013]. Here we use the data of all earlier-analyzed continental samples of the Wuqia Group from both the Kezi (43 samples dated ~41–40 Ma) and Aertashi sections (313 samples from the interval below the disconformity dated as ~41–36 Ma; 140 samples from the interval above dated as ~33–27 Ma) to calculate vertical-axis rotations.

3.1. Rock Magnetic Analyses

Based on previous temperature-dependent rock magnetic analyses (Curie balance and susceptibility bridge) on representative red bed samples [*Bosboom et al.*, 2013], a decrease in magnetization is observed near the Curie temperature of magnetite (~580°C) and more frequently of hematite (~680°C). Previous measurement of the remanent magnetization after stepwise thermal demagnetization in shielded ovens indicates that after progressive removal of an overprint component at temperatures of 100 to 300°C, the characteristic remanent magnetization (ChRM) is composed of a low-temperature component (LTC) and a high-temperature component (HTC). These components are parallel, and both decay toward the origin. In general, the LTC is removed from 350 to 600°C, whereas the HTC is unblocked from 640 to 700°C, supporting the rock magnetic results that magnetite and hematite are the dominant ferromagnetic carriers. For more details on the rock magnetic analyses we refer to *Bosboom et al.* [2013].

3.2. ChRM Direction Analyses

The ChRM directions were calculated from orthogonal plots by application of principal component analysis [*Kirschvink*, 1980]. The line fits were performed on a minimum of four temperature steps. For our rotation analyses we have solely selected from the magnetostratigraphic data set the ChRM data of the highest quality, yielding

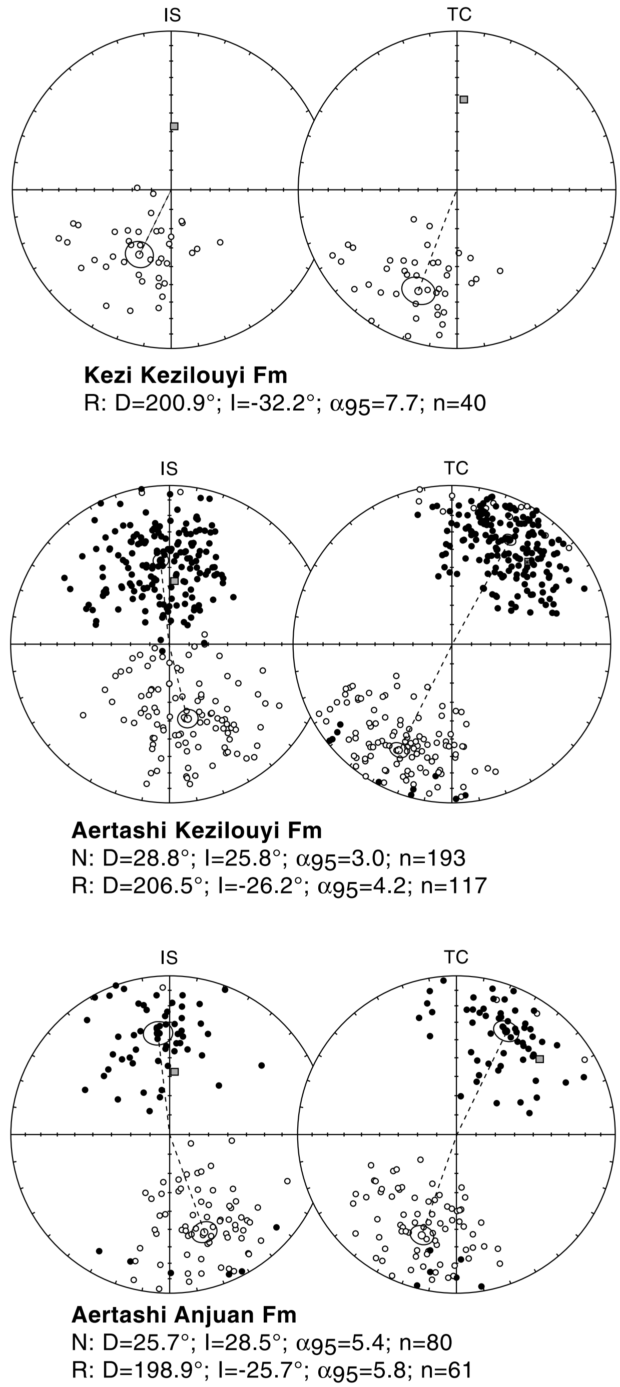

Figure 3. Equal-area plots of the ChRM directions, shown for each section and formation both for in situ (IS) versus tilt-corrected (TC) coordinates. Downward directions are shown as solid symbols, whereas upward directions are shown as open symbols. Fisher means are indicated for normal (*N*) and reversed (*R*) polarities with circles indicating the α_{95} confidence limit. The direction of the present-day normal field is indicated by the grey square for comparison.

unambiguous directions and maximum angular deviations below 15° without forcing directions through the origin. After bedding-tilt correction, the selected directions group in two antipodal normal and reversed clusters on stereographic projections. Fisher statistics (Figure 3) [*Fisher*, 1953] were used to calculate the mean normal and reversed ChRM directions and their α_{95} (95% confidence angle). The outliers and transitional directions positioned more than 45° from the normal and reversed means were iteratively rejected.

Table 1. Paleomagnetic Mean Directions From the Kezilouyi and Anjuan Formations at the Kezi and Aertashi Sections in the Southwest Tarim Basin[a]

Section (Age)	*n*	In Situ (IS) *D* (Deg)	In Situ (IS) *I* (Deg)	Tilt Corrected (TC) *D* (Deg)	Tilt Corrected (TC) *I* (Deg)	*k*	α_{95} (Deg)
Kezi (41–40 Ma) = normal	0						
Kezi (41–40 Ma) = reverse	17			203.9	216.9	11.3	11.1
Kezi (41–40 Ma) = all	17	26.9	54.2			11.9	10.8
Kezi (41–40 Ma) = all	17			23.9	36.9	11.3	11.1
Indeterminate reversals test							
Aertashi (41–36 Ma) = normal	95			32.4	26.8	15.4	3.8
Aertashi (41–36 Ma) = reverse	47			209.4	−31.5	10.7	6.7
Aertashi (41–36 Ma) = all	142	348.7	50.8			12.0	3.6
Aertashi (41–36 Ma) = all	142			31.2	28.3	13.0	3.4
Positive reversals test (classification B); critical angle = 8.0°; normal reverse angle = 5.4°.							
Aertashi (33–27 Ma) = normal	26			29.5	33.9	14.7	10.0
Aertashi (33–27 Ma) = reverse	16			204.3	−39.0	16.0	7.3
Aertashi (33–27 Ma) = all	42	341.2	40.6			15.0	5.9
Aertashi (33–27 Ma) = all	42			26.3	37.2	15.5	5.8
Positive reversals test (classification B); critical angle = 12.1°; normal reverse angle = 6.6°.							

[a]Note: *n* = number of sample characteristic remanent magnetization (ChRM) directions averaged to calculate site mean direction; *D* = declination and *I* = inclination of site mean directions for in situ (geographic) and tilt-corrected (stratigraphic) coordinates; *k* = concentration parameter; α_{95} = angular radius of 95% confidence on mean direction. Averages of site mean directions are given by formation and by polarity (normal and reverse). Reliability is evaluated by the outcome of the reversals test of *McFadden and McElhinny* [1990].

For the Aertashi section, the data was separated into two age bins of ~41–36 Ma and ~33–27 Ma, respectively, below and above the observed disconformity.

3.3. Reliability Tests

The uniform bedding orientation at both sections precludes a fold test, but to assess the nature of the acquired ChRM directions the reversals test of *McFadden and McElhinny* [1990] was applied. The two age bins of the Aertashi section both pass with classification B. This indicates a primary magnetization without secondary bias in directions, thus providing reliable results for rotational analysis. As the red beds of the Kezi section have solely yielded reversed ChRM directions, a reversal test cannot be applied. However, a primary origin is likely based on the consistency in the rock magnetic properties and ChRM directions in comparison to the Aertashi samples and because the ChRM directions in geographic coordinate depart significantly from the present-day field orientation.

4. Results

4.1. Rotational Analyses

To evaluate the direction and magnitude of vertical-axis rotations, we compare our well-dated locality-mean directions to expected directions derived at the locality sites from the Eurasian apparent polar wander path (APWP) of according age from *Torsvik et al*. [2008]. Rotations and flattening have been calculated according to methods of *Butler* [1992]. The mean inclination values are systematically lower than the 59.0 ± 2.5° expected from the Paleogene Eurasian APWP, yielding 21.5 ± 5.1° to 30.7 ± 3.4° of flattening. This can be interpreted as resulting from inclination shallowing during depositional and compaction processes as observed in numerous red beds in Asia [e.g., *Dupont-Nivet et al*., 2002b; *Gilder et al*., 2001].

Observed declinations consistently yield clockwise rotations with respect to expected declinations at both sections (Table 1): 21.6 ± 4.2° in 41 to 36 Ma strata then 17.1 ± 6.5° in 33 to 27 Ma strata at the Aertashi section and 14.2 ± 11.5° in 41 to 40 Ma strata at the Kezi section. These results are statistically indistinguishable given the confidence intervals such that it is not possible to infer if the rotation occurred gradually between 41 and 36 Ma; however, we can infer that most of it occurred after 36 Ma. To better understand the tectonic significance of these rotations and their evolution in time and space, they are discussed below in light of a regional review of previous paleomagnetic results

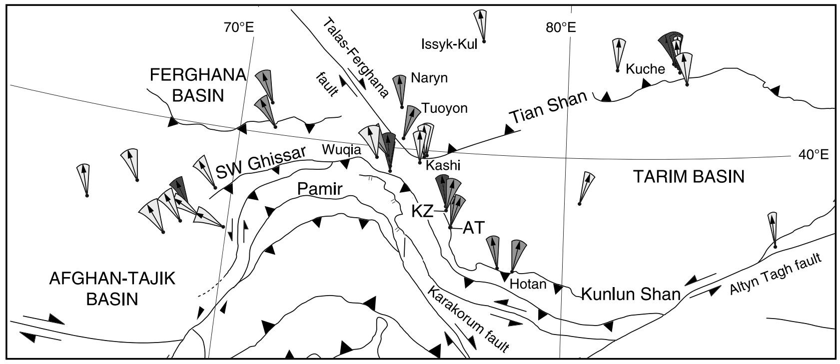

Figure 4. Simplified structural map of the Pamir collision zone (modified from *Cowgill* [2010]) showing the distribution of paleomagnetic rotations from Cretaceous and Cenozoic strata around the Pamir in Central Asia. Rotations and uncertainties are shown with respect to the Eurasian APWP (see Table 2 for complete list and references). Dark grey indicates Cretaceous data, medium grey indicates Paleogene data, and light grey indicates Neogene data. The results of this study are at the Aertashi (AT) and Kezi (KZ) sections.

4.2. Comparison With Previous Paleomagnetic Results Around the Pamir

At the Aertashi section, previous results [*Rumelhart et al*., 1999; *Yin et al*., 2000] indicate low amounts (8.4 ± 5.8°) of clockwise rotation from strata sampled stratigraphically above our own sampling and therefore necessarily younger. According to magnetostratigraphic dating of *Yin et al*. [2002], these rocks have been deposited between ~33 and ~24 Ma implying limited Neogene rotation. Together with our results showing significant clockwise rotations recorded in 41–36 Ma sediments, this suggests that the tectonic mechanism responsible for most of the rotation acquired at the Aertashi section occurred in Oligocene times before ~24 Ma.

To understand whether this rotation is only local or systematically extends regionally we review other results from Cretaceous and younger strata along the eastern Pamir and more generally in the Tarim Basin (Figure 4 and Table 2). Our slightly lower 14.2 ± 11.5° rotation in 41 to 40 Ma strata observed at the Kezi section to the north suggests that clockwise rotations occurred systematically along the West Kunlun Shan with varying degrees of magnitude. However, previous contrasting results have been reported from Cretaceous to Paleogene continental and marine strata at the Yingjisha section only a few kilometers to the north of the Kezi section (Figure 4) [*Chen et al*., 1992]. At this locality, mean declinations are low and yield no significant rotations when compared to the Eurasian APWP. However, the following evidence suggests that this site may be discarded for inferring a regional tectonic mechanism. This result has been previously associated with local structures departing from the regional trend [*Yin et al*., 2000]. In addition, the absence of rotation in this site may also relate to the wholesale and regional remagnetization of the marine strata evidenced previously [*Bosboom et al*., 2013] that would partially bias those data sets. Similarly, *Li et al*. [2013] recently reported results from a section referred to as the Qimugen section which is the same as the Kezi section reported here. These results are mostly marine sediments from the Kashi Group (i.e., from the levels −300 to 250 m in *Li et al*., 2013) that have been shown to be biased by remagnetization [*Bosboom et al*., 2013] yielding erroneously limited amounts of rotation and therefore should be rejected for tectonic analysis. Note that the stratigraphic divisions and the ages reported in *Li et al*. [2013] must be corrected according to the magnetostratigraphic constraints now available in *Bosboom et al.* [2013]. Accordingly, marine sediment reported by *Li et al*. [2013] from the Kashi Group includes the Qimugen, Kalatar, and Wulagen Formations (but not the Bashibulake Formation, which is not present in this part of the basin). *Li et al*. [2013] also report a few paleomagnetic results from the overlying continental red beds of the Wuqia Group. Unfortunately, these results did not yield an interpretable set of directions, and the stratigraphic position of these rocks is not clear such that it is not possible to compare them with our results. In summary, after discarding results likely biased by remagnetizations [*Chen et al*., 1992; *Li et al*., 2013], paleomagnetic studies from the eastern flank of the Pamir indicate systematic clockwise rotations with maximum ~25° magnitude.

By comparison to previous results across the Tarim Basin, it is immediately apparent that these clockwise rotations do not continue systematically into the Tarim Basin. Both senses of rotations are observed in the

Table 2. Review of Paleomagnetic Results From the Tarim Basin Shown for Various Subregions[a]

		Age	Ref.	Site Location		Observed Direction (TC)						Reference Pole				Rotation		
Section	Formation	(Ma)		Lat. (°N)	Long. (°E)	D (Deg)	I (Deg)	α_{95} (Deg)	n		Test ±	Age	Lat. (°N)	Long. (°E)	α_{95} (Deg)	R (Deg)	±	ΔR (Deg)
						Eastern Pamir												
Aertashi	Wuqia Group	<33–24? Ma	1	38.1	76.4	17.6	36.9	5.0	56	s	+f C	30	82.7	152.5	2.8	8.4	±	5.8
Aertashi	Wuqia Group	33–27 Ma	*	38.0	76.6	26.3	37.2	5.8	42	s	A	30	82.7	152.5	2.8	17.1	±	6.5
Aertashi	Wuqia Group	41–36 Ma	*	38.0	76.6	31.2	28.3	3.4	142	s	A	40	82.3	150.5	2.8	21.6	±	4.2
Kezi	Wuqia Group	41–40 Ma	*	38.4	76.4	23.9	36.9	11.1	17	s	n/a	40	82.3	150.5	2.8	14.2	±	11.5
Yingjisha	Yingjisha-Kezilesu	K	2	38.5	76.4	9.6	38.4	8.0	9	S	n/a	100	78.5	179.7	2.7	−4.1	±	8.6
						Altyn Tagh												
Jianglisai		N1	1	38.0	86.5	−1.6	39.6	6.7	28	s	+f C	20	85.0	137.4	3.0	−6.7	±	7.7
						Kuche Basin (Tian Shan)												
Yaha	Kuche-Xiyu	5.3–1.7	3	41.9	83.3	−2.4	54.1	2.4	256	s	A	0	87.6	133.6	3.0	−4.9	±	4.7
Yaha	Jidike-Xiyu	12.6–5.2	4	41.9	83.3	−6.8	43.5	2.6	406	s	+f -r	10	87.2	125.0	2.5	−9.4	±	4.0
Section A	Jidike-Kuche	16.5–5.7	5	42.0	83.3	−2.3	46.1	2.1	66	S	+f A	10	87.2	125.0	2.5	−4.9	±	3.7
Section B	Kumugeliemu-Jidike	29.0–15.5	5	42.0	83.3	6.0	42.8	6.2	15	S	+f C	20	85.0	137.4	3.0	0.3	±	7.6
Kuche Basin	Suweiyi	±N1	6	41.6	83.5	24.6	54.6	10.3	2	S	+f + r	50	79.1	154.2	2.6	10.2	±	14.7
Kuche Basin	Suweiyi	±E3	6	41.6	83.5	2.2	45.3	13.8	3	S	+f + r	50	79.1	154.2	2.6	−12.2	±	16.1
Kuche Basin	Kumugeliemu	±E1–2	6	41.6	83.5	−8.5	39.0	8.9	10	S	+f +r	50	80.9	162.0	2.6	−20.7	±	9.6
Kuche River	Qigu-Kumugeliemu	K	7	42.1	83.1	13.8	39.3	3.8	149	s	+f +r	100	78.5	179.7	2.7	−1.1	±	4.8
Kuche River-Bestantuogela	Kapusaliang Group	K	8	42.1	83.2	16.4	29.3	9.5	21	S	+f C	100	78.5	179.7	2.7	1.5	±	9.2
Kuche Basin	Bashenjiqike	K2	9	42.0	81.6	16.0	39.0	9.0	4	S	+f	75	79.9	171.7	1.5	2.5	±	9.4
Kezilenuer Channel	Bashenjiqike-Kumugeliemu	K1	7	42.1	83.1	−7.1	60.2	15.1	42	s	n/a	70	80.3	181.8	2.7	−19.6	±	25.4
Paicheng	Yageliemu-Kelaza	J3–K1	9	42.0	81.6	22.0	42.0	9.0	6	S	+f	130	75.7	167.7	6.4	2.8	±	11.9
						Kashi Basin (Tian Shan)												
Ganghangou	Atushi-Xiyu	2.2–1.0	10	39.8	76.2	15.9	32.5	10.6	33	s	C	0	87.6	133.6	3.0	13.2	±	10.6
Boguzihe	Atushi-Xiyu	3.6–1.4	10	39.8	76.2	−10.6	43.2	1.9	258	s	A	0	87.6	133.6	3.0	−13.3	±	3.8
North Kashi	Atushi	N2	11	39.6	76.0	−4.3	40.2	9.0	13	S	+f	0	87.6	133.6	3.0	−7.0	±	10.0
North Atushi	Atushi	N2	11	39.8	76.1	−13.1	45.1	7.2	11	S	+f	0	87.6	133.6	3.0	−15.8	±	8.8
North Atushi	Kezilouyi-Pakabulake	N1	11	39.8	76.1	−16.7	44.6	9.6	10	S	+f	10	87.2	125.0	2.5	−19.5	±	11.2
						Tuoyon Basin (Tian Shan)												
Locality A + B	Upper Basalt Series	E1v	12	40.2	75.3	48.4	49.1	6.6	20	S	+f	60	79.0	166.8	2.4	34.2	±	8.5
Tuoyon	Kezilesu Group	K1	13	40.2	75.3	37.9	38.6	6.8	5	S	+f	125	76.3	175.6	6.2	21.1	±	9.3
Tuoyon	Kezilesu Group	K1v	13	40.2	75.3	31.9	49.9	10.6	13	S	+f	125	76.3	175.6	6.2	15.1	±	14.6
						Wuqia area												
East Kulukeqiati	Atushi	N2	11	39.8	74.6	−14.8	50.6	24.3	5	S	+f	0	87.6	133.6	3.0	−17.5	±	32.5
East Kulukeqiati	Kezilouyi-Pakabulake	N1	11	39.8	74.6	−11.9	42.0	7.8	15	S	+f	10	87.2	125.0	2.5	−14.8	±	8.8
West Wuqia	Kashi Group	E2	11	39.8	74.7	−23.1	47.4	11.1	8	S		40	82.3	150.5	2.8	−33.1	±	13.6
Wuqia area	Yingjisha-Kezilesu	K	2	39.5	75.0	10.3	38.6	8.2	18	S	+f	100	78.5	179.7	2.7	−3.4	±	8.8
						Central Tarim and Hotan Basin												
Maza Tagh	Wuqia Group	N1	14	38.5	80.5	24.7	29.4	6.2	30	S	+f	20	85.0	137.4	3.0	19.1	±	6.5
Puska	Kashi Broup	E2	1	37.1	78.4	4.3	24.3	8.4	22	s	+f Cr	50	79.1	154.2	2.6	−9.3	±	7.8
Duwa-Piyaleman	Aertashi-Qimugen	E1	15	37.0	79.0	27.8	30.0	13.3	5	S	+f	60	79.0	166.8	2.4	14.1	±	12.6

Notes to Table 2:

[a]Age of sampled formation given by numbers when magnetostratigraphic control on age span is available or given by epoch notation otherwise (K1 = Early Cretaceous; K2 = Late Cretaceous; E1 = Paleocene; E2 = Eocene; E3 = Oligocene; N1 = Miocene; N2 = Pliocene; v = data from volcanic rocks; ± = age estimated). Lat. = latitude and Long. = longitude of section location; D = declination and I = inclination for tilt-corrected (stratigraphic coordinates); α_{95} = angular radius of 95% confidence on mean direction; n = number of sites (S) or samples (s) used to calculate mean directions; Test refers to the outcome of reversals (r) or fold test (f) as positive (+), negative (−), not applicable (n/a), or the classification (A, B, or C) of the reversals test of *McFadden and McElhinny* [1990]. Reference poles are the Eurasian paleomagnetic poles from *Torsvik et al.* [2008]. Shaded reference pole data indicate that mean poles have been calculated for long age spans of more than 30 Myr. R = vertical-axis rotation (clockwise is positive) and ΔR = 95% confidence limit on rotation. References (Ref.): * = this study; 1, *Rumelhart et al.* [1999]; 2, *Chen et al.* [1992]; 3, *Huang et al.* [2010]; 4, *Charreau et al.* [2006]; 5, *Huang et al.* [2006]; 6, *Fang et al.* [1998]; 7, *Peng et al.* [2006]; 8, *Tan et al.* [2003]; 9, *Li et al.* [1988]; 10, *Chen et al.* [2002]; 11, *Huang et al.* [2009]; 12, *Huang et al.* [2005]; 13, *Gilder et al.* [2003]; 14, *Dupont-Nivet et al.* [2002a]; 15, *Gilder et al.* [1996].

Hotan Basin along the West Kunlun Shan (Puska and Duwa sections) and in central Tarim (Maza Tagh section) that have been attributed equally to either wholesale Tarim block rotation or recent local structures [*Dupont-Nivet et al.*, 2002a; *Gilder et al.*, 1996; *Rumelhart et al.*, 1999; *Yin et al.*, 2000]. Along the left-lateral Altyn Tagh fault little to no rotations are observed locally and regionally [*Dupont-Nivet et al.*, 2002b, 2003; *Dupont-Nivet et al.*, 2004; *Rumelhart et al.*, 1999; *Yin et al.*, 2000]. Along the southern Tian Shan from the Wuqia area to the Kashi and Kuche Basins further east, rotations are predominantly counterclockwise or insignificant and have been associated with Neogene left-lateral transpressive shear along the Tian Shan range itself [*Charreau et al.*, 2006; *Chen et al.*, 2002, 1992; *Fang et al.*, 1998; *Huang et al.*, 2009, 2010; *Li et al.*, 1988; *Peng et al.*, 2006; *Tan et al.*, 2003]. Departing from this general trend are clockwise rotations reported from Cretaceous-Paleocene volcanic rocks in the Tuoyun Basin associated with the right-lateral Talas-Ferghana fault [*Gilder et al.*, 2003; *Huang et al.*, 2005]. In summary, clockwise rotations observed along the eastern Pamir limb do not extend systematically and regionally into the Tarim Basin, where Cenozoic rotations are generally low and associated with local structures (Figure 5).

On the western side of the Pamir salient (Figure 4 and Table 3), Cretaceous to Cenozoic results are strikingly different with systematic counterclockwise rotations extending widely throughout the Afghan-Tajik and Ferghana Basins [*Bazhenov and Mikolaichuck*, 2002; *Bazhenov et al.*, 1994; *Burtman*, 2000; *Pozzi and Feinberg*, 1991; *Thomas et al.*, 1993, 1994]. These rotations show a clear westward decreasing trend ranging from ~ −60° along the Darvaz fault on the eastern Pamir limb to no significant rotation over ~300 km to the west (Figure 5). Structural and kinematic reconstructions show that this trend can be reconciled by the relative displacement and rotation of finite crustal thrust sheets in response to the regional left-lateral shear related to the northward Pamir indentation [*Bourgeois et al.*, 1997; *Thomas et al.*, 1994].

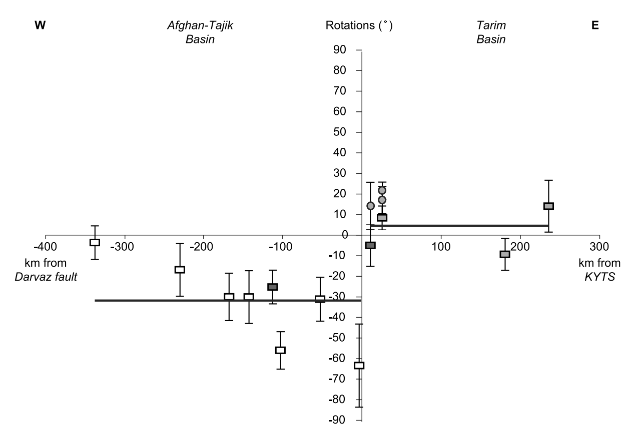

Figure 5. Vertical-axis rotations plotted against approximate east-west distance from the Kashgar-Yecheng transfer system (KYTS) marking the eastern margin of the Pamir and the Darvaz fault marking its western margin. Solid lines indicate the mean observed rotation on either side of the Pamir, showing that the average varies from −32.2° anticlockwise rotation in the Afghan-Tajik Basin on the western side to 6.5° clockwise rotation in the Tarim Basin on the eastern side. As in Figure 5 dark grey indicates Cretaceous data, medium grey indicates Paleogene data, and light grey indicates Neogene data. The results of this study are shown by circles (instead of squares).

In summary, tectonic rotations around the Pamir show a strong asymmetry between regionally extensive systematic counterclockwise rotation in Cretaceous to Neogene strata on the western side of the Pamir contrasting with Oligocene clockwise rotations concentrated along the eastern Pamir limb that do not extend far eastward into the Tarim Basin (Figures 4 and 5).

5. Discussion

The curved geometry of the Pamir has been related to end-member models: (1) rotation by oroclinal bending or radial thrusting of the Pamir arc [*Bazhenov and Burtman*, 1986; *Bazhenov et al.*, 1994; *Robinson et al.*, 2004; *Strecker et al.*, 1995] or (2) transfer faulting induced by opposite shear along the

Table 3. Review of Paleomagnetic Results From Tajikistan and Kyrgyzstan Shown for Various Basins[a]

	Age	Ref.	Site Location		Observed Direction (TC)						Reference Pole				Rotation		
Section	(Ma)		Lat. (°N)	Long. (°E)	*D* (Deg)	*I* (Deg)	α_{95} (Deg)	*n*		Test ±	Age	Lat. (°N)	Long. (°E)	α_{95} (Deg)	*R* (Deg)	±	Δ*R* (Deg)
							Afghan-Tajik Basin (Tajikistan)										
Kalinabad	N1	1	38.0	69.0	−50.0	33.0	9.0	13	L	n/a	20	85.0	137.4	3.0	−56.0	±	9.1
Aksu	N1	1	38.0	68.6	−24.0	33.0	13.0	5	L	n/a	20	85.0	137.4	3.0	−30.1	±	12.8
Pyryagata	N1	1	37.7	68.3	−24.0	30.0	12.0	6	L	+ (*f*)	20	85.0	137.4	3.0	−30.0	±	11.5
Pulkhakim	N1	1	39.1	67.5	−11.0	35.0	13.0	10	L	+ (*f*) + (*r*)	20	85.0	137.4	3.0	−17.2	±	13.1
Tukaynaron	E3-			N1	1	38.8	69.6								−25.0		30.0
L	+ (*f*) + (*r*)		11.0	10	20	85.0	137.4			3.0					−31.1	±	10.7
South Darvaz	E2-			N1	1	37.7	68.1								−56.0		32.0
21.0	3	L	+ (*r*)	25	84.1	147.1	2.8								−63.4	±	20.2
Nurek Dam + Nurek Pass + Gissar + Ragoon	K1	2	38.3	68.9	−9.5	55.4	4.0	53	s	+ (*f*)	125	76.3	175.6	6.2	−25.2	±	8.2
							Aksay Basin (Kyrgyzstan)										
Tekelik	E2-3	3			14.6	54.0	3.8	18	L	+ (*f*)	40	81.7	154.5	2.8	11.0	±	5.7
							Chatkal Basin (Kyrgyzstan)										
Chatkal	E	4	41.7	71.2	−8.0	42.0	9.0	10	L	n/a	40	82.3	150.5	2.8	−18.3	±	10.2
							Ferghana Basin (Kyrgyzstan)										
Tash-Kumyr + Ala-Buka + South Ferghana	E	4	41.1	71.2	−18.0	34.0	9.0	9	L	+ (*f*) + (*r*)	40	82.3	150.5	2.8	−28.2	±	9.2
							Issyk-Kul Basin (Kyrgyzstan)										
Dzhety-	E2-			N1	4	42.4	77.1			2.0		49.0	6.0	13	L	+	(*f*)
Ogyuz + Karakoo + Toru Aygyr		30	82.7	152.5													2.8
−7.8	±	+		(*r*)	8.0												
							Naryn Basin (Kyrgyzstan)										
Karabulan + Djaman-Davan + Makmal	E	4	41.2	74.7	5.0	37.0	11.0	16	L	+ (*f*) + (*r*)	40	82.3	150.5	2.8	−5.2	±	11.5

[a]See note of Table 2 for explanation. References: 1, *Thomas et al.* [1994]; 2, *Pozzi and Feinberg* [1991]; 3, *Bazhenov and Mikolaichuck* [2002]; 4, *Thomas et al.* [1993].

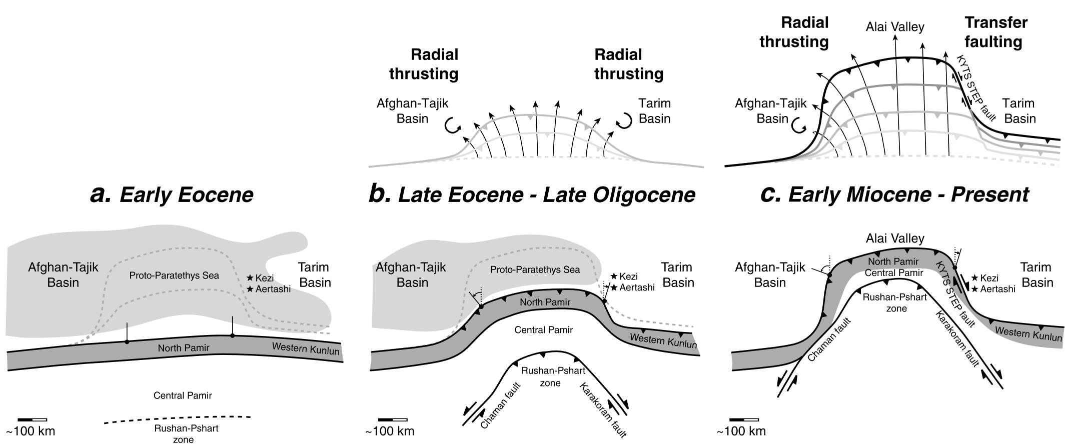

Figure 6. Proposed tectonic and paleogeographic evolution of the Pamir salient (modified after *Cowgill* [2010]), based upon results of this study and previous studies of the proto-Paratethys Sea [*Bosboom*, 2013; *Burtman*, 2000; *Burtman et al.*, 1996; *Coutand et al.*, 2002; *Lan and Wei*, 1995; *Tang et al.*, 1989]. The paleogeographic evolution is shown in the lower graphs with the approximate paleogeographic extent of the sea shaded in light grey for the (a) Early Eocene and (b) before its final retreat in the Late Eocene. The upper graphs show the corresponding kinematic models. The Pamir evolved symmetrically with radial thrusting causing rotation on both sides until the Late Oligocene. In the Late Oligocene to Early Miocene, deformation became asymmetric with ceased clockwise rotation in the Tarim Basin and continued anticlockwise rotation on the western side in the Afghan-Tajik Basin. This change is attributed to the initiation of slip along the Kashgar-Yecheng transfer system (KYTS) along the eastern Pamir in response to slab tear of the underriding Alai plate. See the discussion for a complete overview of this proposed evolution.

eastern (sinistral) and western (dextral) margins of the Pamir [*Burtman and Molnar*, 1993; *Searle*, 1996]. A hybrid of the above-mentioned end-member models has been recently proposed by *Cowgill* [2010]. This hybrid model involves northwest directed radial thrusting on the Pamir's western flank and transpressional dextral slip transfer faulting along the Kashgar-Yecheng transfer system (KYTS) on its eastern flank. This model is supported by *Li et al*. [2013] albeit based on data biased by remagnetization, yielding erroneously no rotation of the eastern flank since Paleocene times. In contrast, our reliable results indicate a regional Oligocene clockwise rotation and suggest this rotation mostly ceased in Neogene times. Our results thus imply a two-stage evolution that can be reconciled by the following model (Figure 6). After the Early Eocene initiation of the Pamir indentation associated with the Indo-Asia collision, the deformation propagated from Late Eocene to Late Oligocene into a proto Tajik-Tarim foreland basin inducing symmetric rotations by radial thrusting on either side of the nascent Pamir salient. By Early Miocene time, the observed asymmetry in the pattern of rotations indicates that radial thrusting did not continue east of the Pamir as it did to the west but was replaced by a mechanism such as strike-slip transfer faulting with limited distributed shear.

This model is consistent in time with the recently dated paleogeographic evolution of the proto-Paratethys Sea (Figure 6), involving its stepwise westward retreat in the Eocene forced by short-term eustacy and long-term tectonism related to the Pamir indentation [*Bosboom et al*., 2013, 2011; *Bosboom*, 2013]. In the Early Eocene marine deposits had their maximum extent reaching far eastward into the Tarim Basin [*Burtman*, 2000; *Burtman et al*., 1996; *Lan and Wei*, 1995; *Tang et al*., 1989]. The maximum extent of each of the next incursions reached successively less far into the Tarim Basin; the last one reaching only the westernmost Tarim Basin in Late Eocene times [*Bosboom*, 2013]. The complete disappearance of the sea from Central Asia is poorly constrained to the Oligocene, followed by mostly continental deposition in Late Oligocene and Early Miocene times [e.g., *Burtman*, 2000; *Burtman et al*., 1996; *Coutand et al*., 2002]. This suggests that the observed Oligocene rotations may be related to tectonism propagating northward after the Late Eocene regional sea retreat and disappearance. After the Oligocene, a major right-lateral strike-slip system is reported to start in the Early Miocene along the eastern Pamir [*Sobel and Dumitru*, 1997; *Sobel et al*., 2011]. This is supported locally at Aertashi by the initiation of proximal coarse-grained clastic deposition from ~24 Ma [*Yin et al*., 2002] interpreted as a response to the initial dextral slip between the Pamir and the Tarim Basin [*Cowgill*, 2010]. Neogene decoupling of the Pamir from Tarim along this major strike-slip system is corroborated by the limited rotations accumulated in the Neogene with no regional consistency east of the Pamir into the Tarim Basin. This probably also corresponds to an important geodynamic change consistent with Early Miocene ages of exhumation and deformation in the eastern Pamir, Western Kunlun Shan, and Tian Shan [e.g., *De Grave et al*., 2012; *Sobel and Dumitru*, 1997; *Sobel et al*., 2006].

Finally, our results are consistent in time and space with the recently proposed intracontinental subduction models of Pamir evolution [*Negredo et al*., 2007; *Sobel et al*., 2013]. In these models, Eocene break off of the north dipping Indian slab associated with the Indo-Asia collision is followed by a period of intense deformation related to subduction inversion and the initiation of a new intracontinental south dipping subduction at ~25 Ma [*Negredo et al*., 2007]. This is in good agreement with the observed Oligocene rotations with radial thrusting on either side of the nascent Pamir salient. *Sobel et al*. [2011, 2013] further suggest that the Pamir indentation could have been driven by roll back of the south dipping slab starting at ~25 Ma with a curved slab on its western flank and the initiation of a slab tear (or STEP, Subduction-Transform Edge Propagator as defined by *Govers and Wortel* [2005]) along its eastern flank linked to the dextral KYTS (Figure 6). This is consistent with the observed asymmetric distribution rotations starting in Miocene times. On the western flank, regionally distributed counterclockwise rotations would have continued into the Miocene in response to the retreating curved slab. On the eastern flank, clockwise rotations would have stopped after the Oligocene when the STEP initiated yielding a strike-slip system with limited distributed shear.

6. Conclusions

Arc-shaped ranges may result from a wide array of potential tectonic mechanisms yielding characteristic patterns of vertical-axis rotations that can be quantified using paleomagnetism [*Weil and Sussman*, 2004]. The case of the Pamir range is particularly interesting because of the asymmetry in observed rotations on either side of the arc resulting from contrasting mechanisms but yielding a seemingly symmetric shape in map view. Another peculiar aspect, suggested here, is the shift of the rotational pattern from symmetric to asymmetric in the Late Oligocene to Early Miocene that enables us to identify a major change in geodynamic regime. This shows generally that regular arcuate structures may in fact be the result of a protracted history and cannot be assumed to have evolved regularly since inception. The analysis of vertical-axis rotations using paleomagnetism provides a tool to quantify the evolution of arcuate belts in time that can be particularly useful to constrain geodynamic models of these structures [e.g., *Schellart and Rawlinson*, 2010].

Acknowledgments
This project was funded by the Netherlands Organization for Scientific Research (NWO) with grants to Roderic Bosboom and Guillaume Dupont-Nivet. We also acknowledge funding from the Cai Yuanpei program of the French ministries of foreign affairs and of higher education and research and the Chinese ministry of education. We would like to thank Cor Langereis, Wout Krijgsman, Arjen Grothe, Beibei Zhu, and Ziya Yang for their contributions in the field. Tom Mullender and Mark Dekkers are thanked for their assistance in the paleomagnetic laboratory.

We thank Alex Robinson and an anonymous reviewer for detailed and thoughtful comments.

References

Amidon, W. H., and S. A. Hynek (2010), Exhumational history of the north central Pamir, *Tectonics*, *29*, TC5017, doi:10.1029/2009TC002589.

Bazhenov, M. L., and A. V. Mikolaichuck (2002), Paleomagnetism of Paleogene basalts from the Tien Shan, Kyrgyzstan: Rigid Eurasia and dipole geomagnetic field, *Earth Planet. Sci. Lett.*, *195*, 155–166, doi:10.1016/S0012-821X(01)00586-6.

Bazhenov, M. L., and V. S. Burtman (1986), Tectonics and paleomagnetism of structural arcs of the Pamir-Punjab syntaxis, *J. Geodyn.*, *5*(3), 383–396, doi:10.1016/0264-3707(86)90017-7.

Bazhenov, M. L., H. Perroud, A. Chauvin, V. S. Burtman, and J. C. Thomas (1994), Paleomagnetism of Cretaceous red beds from Tadzhikistan and Cenozoic deformation due to India-Eurasia collision, *Earth Planet. Sci. Lett.*, *124*, 1–18, doi:10.1016/SSDI0012-821X(94)00072-7.

Bershaw, J., C. N. Garzione, L. Schoenbohm, G. Gehrels, and L. Tao (2012), Cenozoic evolution of the Pamir plateau based on stratigraphy, zircon provenance, and stable isotopes of foreland basin sediments at Oytag (Wuyitake) in the Tarim Basin (west China), *J. Asian Earth Sci.* *44*, 136–148, doi:10.1016/j.jseaes.2011.04.020.

Bosboom, R. E. (2013), *Paleogeography of the Central Asian Proto-Paratethys Sea in the Eocene*, 225 pp., Utrecht University, Utrecht.

Bosboom, R. E., G. Dupont-Nivet, A. J. P. Houben, H. Brinkhuis, G. Villa, O. Mandic, M. Stoica, W.-J. Zachariasse, Z. Guo, and C. Li (2011), Late Eocene sea retreat from the Tarim Basin (West China) and concomitant Asian paleoenvironmental change, *Palaeogeogr. Palaeoclimatol. Palaeoecol.*, *299*, 385–398, doi:10.1016/j.palaeo.2010.11.019.

Bosboom, R., et al. (2013), Linking Tarim Basin sea retreat (west China) and Asian aridification in the Late Eocene, *Basin Research*, doi:10.1111/bre.12054, in press.

Bosboom, R. E., H. A. Abels, C. Hoorn, B. C. J. van den Berg, Z. Guo, and G. Dupont Nivet (2014), Aridification in continental Asia after the Middle Eocene Climatic Optimum (MECO), *Earth Planet. Sci. Lett.*, *389*, pp. 34–42.

Bourgeois, O., P. R. Cobbold, D. Rouby, J.–C. Thomas, and V. Shein (1997), Least squares restoration of Tertiary thrust sheets in map view, Tajik depression, central Asia, *J. Geophys. Res.*, *102*(B12), 27,553–27,527,27573, doi:10.1029/97JB02477.

Bureau of Geology and Mineral Resources of Xinjiang Uygur Autonomous Region (1993), *Regional Geology of Xinjiang Uygur Autonomous Region*, Geological House, Beijing.

Burtman, V. S. (2000), Cenozoic crustal shortening between the Pamir and Tien Shan and a reconstruction of the Pamir–Tien Shan transition zone for the Cretaceous and Palaeogene, *Tectonophysics*, *319*(2), 69–92, doi:10.1016/S0040-1951(00)00022-6.

Burtman, V. S., and P. Molnar (1993), Geological and geophysical evidence for deep subduction of continental crust beneath the Pamir, *Geol. Soc. Am. Special Pap.*, *281*, 1–76.

Burtman, V. S., S. F. Skobelev, and P. Molnar (1996), Late Cenozoic slip on the Talas-Ferghana fault, the Tien Shan, central Asia, *Geol. Soc. Am. Bull.*, *108*(8), 1004–1021, doi:10.1130/0016-7606(1996)108<1004:LCSOTT>2.3.CO;2.

Butler, R. F. (1992), *Paleomagnetism: Magnetic Domains to Geologic Terranes*, 238 pp., Blackwell Scientific Publications, Boston.

Charreau, J., Y. Chen, S. Gilder, S. Dominguez, J.-P. Avouac, S. Sen, D. Sun, Y. Li, and W.-M. Wang (2005), Magnetostratigraphy and rock magnetism of the Neogene Kuitun He section (northwest China): Implications for Late Cenozoic uplift of the Tianshan mountains, *Earth Planet. Sci. Lett.*, *230*(1–2), 177–192, doi:10.1016/j.epsl.2004.11.002.

Charreau, J., S. Gilder, Y. Chen, S. Dominguez, J. P. Avouac, S. Sen, and M. Jolivet (2006), Magnetostratigraphy of the Yaha section, Tarim Basin (China): 11 Ma acceleration in erosion and uplift of the Tianshan Mountains, *Geology*, *34*(3), 181–184, doi:10.1130/G22106.1.

Chen, J., D. W. Burbank, K. M. Scharer, E. Sobel, J. Yin, C. Rubin, and R. Zhao (2002), Magnetochronology of the upper cenozoic strata in the Southwestern Chinese Tian Shan: Rates of Pleistocene folding and thrusting, *Earth Planet. Sci. Lett.*, *195*(1–2), 113–130.

Chen, Y., J. P. Cogné, and V. Courtillot (1992), New Cretaceous paleomagnetic results from the Tarim basin, northwestern China, *Earth Planet. Sci. Lett.*, *114*(1), 17–38, doi:10.1016/0012-821X(92)90149-P.

Coutand, I., M. R. Strecker, R. Arrowsmith, G. Hilley, R. C. Thiede, A. Korjenkov, and M. Omuraliev (2002), Late Cenozoic tectonic development of the intramontane Alai Valley, (Pamir-Tien Shan region, central Asia): An example of intracontinental deformation due to the Indo-Eurasia collision, *Tectonics*, *21*(6), 3-1–3-19, doi:10.1029/2002TC001358.

Cowgill, E. (2010), Cenozoic right-slip faulting along the eastern margin of the Pamir salient, northwestern China, *Geol. Soc. Am. Bull.*, *122*(1–2), 145–161, doi:10.1130/B26520.1.

De Grave, J., S. Glorie, A. Ryabinin, F. Zhimulev, M. M. Buslov, A. Izmer, M. Elburg, and F. Vanhaecke (2012), Late Palaeozoic and Meso-Cenozoic tectonic evolution of the Southern Kyrgyz Tien Shan: Constraints from multi-method thermochronology in the Trans-Alai, Turkestan-Alai Section and the Southeastern Ferghana Basin, *J. Asian Earth Sci.*, *44*, 149–168, doi:10.1016/j.jseaes.2011.04.019.

Dupont-Nivet, G., Z. Guo, R. F. Butler, and C. Jia (2002a), Discordant paleomagnetic direction in Miocene rocks from the central Tarim Basin: Evidence for local deformation and inclination shallowing, *Earth Planet. Sci. Lett.*, *199*(3–4), 473–482, doi:10.1016/S0012-821X(02)00566-6.

Dupont-Nivet, G., R. F. Butler, A. Yin, and X. Chen (2002b), Paleomagnetism indicates no Neogene rotation of the Qaidam Basin in North Tibet during Indo-Asian Collision, *Geology*, *30*(3), 263–266, doi:10.1130/0091-7613(2002).

Dupont-Nivet, G., R. F. Butler, A. Yin, and X. Chen (2003), Paleomagnetism indicates no Neogene rotation of the Northeastern Tibetan plateau, *J. Geophys. Res.*, *108*(B8), 2386, doi:10.1029/2003JB002399.

Dupont-Nivet, G., R. F. Butler, A. Yin, D. Robinson, Y. Zhang, W. S. Qiao, and J. Melosh (2004), Concentration of crustal displacement along a weak Altyn Tagh fault: Evidence from paleomagnetism of the northern Tibetan Plateau, *Tectonics*, *23*, TC1020, doi:10.1029/2002TC001397.

Fang, D., P. Wang, Z. Shen, and X. Tan (1998), Cenozoic paleomagnetic results and phanerozoic apparent polar wandering path of Tarim Block, *Sci. Chin. Ser. D*, *41*(2), 105–112, doi:10.1007/BF02984518.

Fisher, R. A. (1953), Dispersion on a sphere, *Proc. R. Soc. London Ser. A Math. Phys. Sci.*, *217*(1130), 295–305, doi:10.1098/rspa.1953.0064.

Gao, Z., K. Chen, and J. Wei (2000), *The Lithostratigraphic Dictionary of China*, 627 pp., Press of Geological University, Beijing.

Gilder, S., X. Zhao, R. Coe, Z. Meng, V. Courtillot, and J. Besse (1996), Paleomagnetism and tectonics of the southern Tarim Basin, northwestern China, *J. Geophys. Res.*, *101*(B10), 22,015–22,031, doi:10.1029/96JB01647.

Gilder, S., Y. Chen, and S. Sen (2001), Oligo-Miocene magnetostratigraphy and rock magnetism of the Xishuigou section, Subei (Gansu Province, western China) and implications for shallow inclinations in central Asia, *J. Geophys. Res.*, *106*(B12), 30,505–30,522, doi:10.1029/2001JB000325.

Gilder, S., Y. Chen, J.-P. Cogne, X. Tan, V. Courtillot, D. Sun, and Y. Li (2003), Paleomagnetism of Upper Jurassic to Lower Cretaceous volcanic and sedimentary rocks from the western Tarim Basin and implications for inclination shallowing and absolute dating of the M-0 (ISEA?) chron, *Earth Planet. Sci. Lett.*, *206*(3–4), 587–600, doi:10.1016/S0012-821X(02)01074-9.

Govers, R., and M. J. R. Wortel (2005), Lithosphere tearing at STEP faults: Response to edges of subduction zones, *Earth Planet. Sci. Lett.*, *236*(1), 505–523, doi:10.1016/j.epsl.2005.03.022.

Gradstein, F. M., J. G. Ogg, M. Schmitz, and G. Ogg (2012), *A Geological Time Scale 2012*, vol. 1 and 2, 1144 pp., Elsevier, Amsterdam.

Graham, S. A., C. P. Chamberlain, Y. J. Yue, B. D. Ritts, A. D. Hanson, T. W. Horton, J. R. Waldbauer, M. A. Poage, and X. Feng (2005), Stable isotope records of Cenozoic climate and topography, Tibetan plateau and Tarim basin, *Am. J. Sci.*, *305*(2), 101–118, doi:10.2475/ajs.305.2.101.

Hao, Y. C., and X. L. Zeng (1984), On the evolution of the west Tarim gulf from Mesozoic to Cenozoic in terms of characteristics of foraminiferal fauna, *Acta Micropalaeontologica Sin.*, *1*(1), 1–13.

Heermance, R. V., J. Chen, D. W. Burbank, and C. Wang (2007), Chronology and tectonic controls of Late Tertiary deposition in the southwestern Tian Shan foreland, NW China, *Basin Res.*, *19*(4), 599–632, doi:10.1111/j.1365-2117.2007.00339.x.

Hendrix, M. S., S. A. Graham, A. R. Carroll, E. R. Sobel, C. L. Mcknight, B. J. Schulein, and Z. Wang (1992), Sedimentary record and climatic implications of recurrent deformation in the Tian Shan: Evidence from Mesozoic strata of the north Tarim, south Junggar, and Turpan basins, northwest China, *Geol. Soc. Am. Bull.*, *104*(1), 53–79, doi:10.1130/0016-7606(1992)104<0053:SRACIO>2.3.CO;2.

van Hinsbergen, D. J. J., P. C. Lippert, G. Dupont-Nivet, N. McQuarrie, P. V. Doubrovine, W. Spakman, and T. H. Torsvik (2012), Greater India Basin hypothesis and a two-stage Cenozoic collision between India and Asia, *Proc. Natl. Acad. Sci. U. S. A.*, *109*(20), 7659–7664, doi:10.1073/pnas.1117262109.

Huang, B., J. D. A. Piper, Y. Wang, H. He, and R. Zhu (2005), Paleomagnetic and geochronological constraints on the post-collisional northward convergence of the southwest Tian Shan, NW China, *Tectonophysics*, *409*(1–4), 107–124, doi:10.1016/j.tecto.2005.08.018.

Huang, B., J. D. A. Piper, S. Peng, T. Liu, Z. Li, Q. Wang, and R. Zhu (2006), Magnetostratigraphic study of the Kuche Depression, Tarim Basin, and Cenozoic uplift of the Tian Shan Range, Western China, *Earth Planet. Sci. Lett.*, *251*(3–4), 346–364, doi:10.1016/j.epsl.2006.09.020.

Huang, B., J. D. A. Piper, and R. Zhu (2009), Paleomagnetic constraints on neotectonic deformation in the Kashi depression of the western Tarim Basin, NW China, *Int. J. Earth Sci.*, *98*(6), 1469–1488, doi:10.1007/s00531-008-0401-5.

Huang, B., J. D. A. Piper, Q. Qiao, H. Wang, and C. Zhang (2010), Magnetostratigraphic and rock magnetic study of the Neogene upper Yaha Section, Kuche Depression (Tarim Basin): Implications to formation of the Xiyu Conglomerate Formation, NW China, *J. Geophys. Res.*, *115*, B01101, doi:10.1029/2008JB006175.

Jia, C., G. Wei, L. Wang, D. Jia, and Z. Guo (1997), *Tectonic characteristics and petroleum, Tarim basin, China*, 295 pp., Petroleum Industry Press, Beijing.

Jia, C., S. Zhang, and S. Wu (2004), *Stratigraphy of the Tarim Basin and Adjacent Areas*, 540 pp., Science Press, Beijing.

Kent-Corson, M. L., B. D. Ritts, G. Zhuang, P. M. Bovet, S. A. Graham, and C. Page Chamberlain (2009), Stable isotopic constraints on the tectonic, topographic, and climatic evolution of the northern margin of the Tibetan Plateau, *Earth Planet. Sci. Lett.*, *282*(1–4), 158–166, doi:10.1016/j.epsl.2009.03.011.

Kirschvink, J. L. (1980), The least-square line and plane and the analysis of paleomagnetic data, *Geophys. J. R. Astron. Soc.*, *62*, 699–718.

Lan, X., and J. Wei (Eds) (1995), *Late Cretaceous-Early Tertiary Marine Bivalve Fauna From the Western Tarim Basin*, 212 pp., Chinese Science House, Beijing.

Li, Y., Z. Zhang, M. McWilliams, R. Sharps, Y. Zhai, Y. Li, Q. Li, and A. Cox (1988), Mezosoic paleomagnetic results of the Tarim craton: Tertiary relative motion between China and Siberia?, *Geophys. Res. Lett.*, *15*(3), 217–220, doi:10.1029/GL015i003p00217.

Li, Z., L. Ding, P. C. Lippert, and H. Wei (2013), Paleomagnetic constraints on the Cenozoic kinematic evolution of the Pamir plateau from the Western Kunlun Shan foreland, *Tectonophysics*, *603*, 257–271, doi:10.1016/j.tecto.2013.05.040.

Mao, S., and G. Norris (1988), *Late Cretaceous-Early Tertiary Dinoflagellates and Acritarchs From the Kashi Area, Tarim Basin, Xinjiang Province, China*, 93 pp., Royal Ontario Museum, Toronto.

McFadden, P. L., and M. W. McElhinny (1990), Classification of the reversal test in palaeomagnetism, *Geophys. J. Int.*, *103*(3), 725–729, doi:10.1111/j.1365-246X.1990.tb05683.x.

Negredo, A. M., A. Replumaz, A. Villasenor, and S. Guillot (2007), Modeling the evolution of continental subduction processes in the Pamir-Hindu Kush region, *Earth Planet. Sci. Lett.*, *259*(1–2), 212–225, doi:10.1016/j.epsl.2007.04.043.

Peng, S., Z. Li, B. Huang, T. Liu, and Q. Wang (2006), Magnetostratigraphic study of Cretaceous depositional succession in the northern Kuqa Depression, Northwest China, *Chinese Sci. Bull.*, *51*(1), 97–107, doi:10.1007/s11434-005-0340-5.

Pozzi, J. P., and H. Feinberg (1991), Paleomagnetism in the Tajikistan: Continental shortening of European margin in the Pamirs during Indian Eurasian collision, *Earth Planet. Sci. Lett.*, *103*(1–4), 365–378, doi:10.1016/0012-821X(91)90173-F.

Ritts, B. D., Y. Yue, S. A. Graham, E. R. Sobel, O. A. Abbink, and D. Stockli (2008), From sea level to high elevation in 15 million years: Uplift history of the northern Tibetan Plateau margin in the Altun Shan, *Am. J. Sci.*, *308*(5), 657–678, doi:10.2475/05.2008.01.

Robinson, A. C., A. Yin, C. E. Manning, T. M. Harrison, S.–. H. Zhang, and X.-F. Wang (2004), Tectonic evolution of the northeastern Pamir: Constraints from the northern portion of the Cenozoic Kongur Shan extensional system, western China, *Geol. Soc. Am. Bull.*, *116*(7–8), 953–973, doi:10.1130/B25375.1.

Robinson, D. M., G. Dupont-Nivet, G. E. Gehrels, and Y. Zhang (2003), The Tula Uplift, northwestern China: Evidence for regional tectonism of the northern Tibetan Plateau during Late Mesozoic–Early Cenozoic time, *Geol. Soc. Am. Bull.*, *115*(1), 35–47, doi:10.1130/0016-7606(2003)115<0035:TTUNCE>2.0.CO;2.

Rumelhart, P. E. (2000), Cenozoic vertical-axis rotation of the Altyn Tagh fault system, *Geology*, *28*(5), 480–480.

Rumelhart, P. E., A. Yin, E. Cowgill, R. F. Butler, Q. Zhang, and X.-F. Wang (1999), Cenozoic vertical-axis rotation of the Altyn Tagh fault system, *Geology*, *27*(9), 819–822, doi:10.1130/0091-7613(1999)027<0819:CVAROT>2.3.CO;2.

Schellart, W. P., and N. Rawlinson (2010), Convergent plate margin dynamics: New perspectives from structural geology, geophysics and geodynamic modelling, *Tectonophysics*, *483*(1–2), 4–19, doi:10.1016/j.tecto.2009.08.030.

Searle, M. P. (1996), Geological evidence against large-scale pre-Holocene offsets along the Karakorum Fault: Implications for the limited extrusion of the Tibetan plateau, *Tectonics*, *15*(1), 171–186, doi:10.1029/95TC01693.

Sippl, C., B. Schurr, X. Yuan, J. Mechie, F. M. Schneider, M. Gadoev, S. Orunbaev, I. Oimahmadov, C. Haberland, and U. Abdybachaev (2013), Geometry of the Pamir-Hindu Kush intermediate-depth earthquake zone from local seismic data, *J. Geophys. Res. Solid Earth*, *118*, 1438–1457, doi:10.1002/jgrb.50128.

Sobel, E. R., and T. A. Dumitru (1997), Thrusting and exhumation around the margins of the western Tarim basin during the India-Asia collision, *J. Geophys. Res.*, *102*(B3), 5043–5063, doi:10.1029/96JB03267.

Sobel, E. R., J. Chen, and R. V. Heermance (2006), Late Oligocene–Early Miocene initiation of shortening in the Southwestern Chinese Tian Shan: Implications for Neogene shortening rate variations, *Earth Planet. Sci. Lett.*, *247*(1–2), 70–81, doi:10.1016/j.epsl.2006.03.048.

Sobel, E. R., L. M. Schoenbohm, J. Chen, R. Thiede, D. F. Stockli, M. Sudo, and M. R. Strecker (2011), Late Miocene–Pliocene deceleration of dextral slip between Pamir and Tarim: Implications for Pamir orogenesis, *Earth Planet. Sci. Lett.*, *304*(3–4), 369–378, doi:10.1016/j.epsl.2011.02.012.

Sobel, E. R., J. Chen, L. M. Schoenbohm, R. Thiede, D. F. Stockli, M. Sudo, and M. R. Strecker (2013), Oceanic-style subduction controls Late Cenozoic deformation of the Northern Pamir orogen, *Earth Planet. Sci. Lett.*, *363*, 204–218, doi:10.1016/j.epsl.2012.12.009.

Strecker, M. R., W. Frisch, M. W. Hamburger, L. Ratchbacher, S. Semiletkin, A. Zamoruyev, and N. Sturchio (1995), Quaternary deformation in the eastern Pamir, Tadzhikistan and Kygyzstan, *Tectonics*, *14*(5), 1061–1079, doi:10.1029/95TC00927.

Tan, X., K. P. Kodama, H. Chen, D. Fang, D. Sun, and Y. Li (2003), Paleomagnetism and magnetic anisotropy of Cretaceous red beds from the Tarim basin, northwest China: Evidence for a rock magnetic cause of anomalously shallow paleomagnetic inclinations from Central Asia, *J. Geophys. Res.*, *108*(B2), 2107, doi:10.1029/2001JB001608.

Tang, T., H. Yang, X. Lan, C. Yu, Y. Xue, Y. Zhang, L. Hu, S. Zhong, and J. Wei (1989), *Marine Late Cretaceous and Early Tertiary Stratigraphy and Petroleum Geology in Western Tarim Basin, China*, 141 pp., Science Press, Beijing.

Thomas, J.–C., H. Perroud, P. R. Cobbold, M. L. Bazhenov, V. S. Burtman, A. Chauvin, and I. S. Sadybakasov (1993), A paleomagnetic study of Tertiary formations from the Kyrgyz Tien-Shan and its tectonic implications, *J. Geophys. Res.*, *98*(B6), 9571–9589, doi:10.1029/92JB02912.

Thomas, J.–C., A. Chauvin, D. Gapais, M. L. Bazhenov, H. Perroud, P. R. Cobbold, and V. S. Burtman (1994), Paleomagnetic evidence for Cenozoic block rotations in the Tadjik depression (Central Asia), *J. Geophys. Res.*, *99*(B8), 15,141–15,160, doi:10.1029/94JB00901.

Tian, Z., G. Chai, and Y. Kang (1989), Tectonic evolution of the Tarim basin, in *Chinese Sedimentary Basins*, edited by X. Zhu, pp. 33–42 , Elsevier, Amsterdam.

Torsvik, T. H., R. D. Muller, R. Van der Voo, B. Steinberger, and C. Gaina (2008), Global plate motion frames: Toward a unified model, *Rev. Geophys.*, *46*, RG3004, doi:10.1029/2007RG000227.

Wei, H.–. H., Q.-R. Meng, L. Ding, and Z.-Y. Li (2013), Tertiary evolution of the western Tarim basin, northwest China: A tectono-sedimentary response to northward indentation of the Pamir salient, *Tectonics*, *32*, 558–575, doi:10.1002/tect.20046.

Weil, A. B., and A. J. Sussman (2004), Classifying curved orogens based on timing relationships between structural development and vertical-axis rotations, *Orogenic curvature integrating paleomagnetic struct. analyses*, *383*, 1–16.

Yang, H., X. Jiang, and S. Lin (1995), *Late Cretaceous–Early Tertiary ostracod fauna from western Tarim Basin, south Xinjiang, China*, 173 pp., Science Press, Beijing.

Yang, Y., and M. Liu (2002), Cenozoic deformation of the Tarim plate and the implications for mountain building in the Tibetan plateau and the Tian Shan, *Tectonics*, *21*(6), 1059, doi:10.1029/2001TC001300.

Ye, D., et al. (1996), *Tertiary in Petroliferous Regions of China*, 375 pp., Petroleum Industry Press, Beijing.

Yin, A., and M. T. Harrison (2000), Geologic evolution of the Himalayan-Tibetan orogen, *Annu. Rev. Earth Planet. Sci.*, *28*, 211–280, doi:10.1146/annurev.earth.28.1.211.

Yin, A., Z. Yang, R. F. Butler, Y. Otofuji, P. E. Rumelhart, and E. Cowgill (2000), Correction of "Cenozoic vertical-axis rotation of the Altyn Tagh fault system" by P. E. Rumelhart et al., Geology, v.27, p. 819–822, September 1999, *Geology*, *28*(5), 480.

Yin, A., et al. (2002), Tectonic history of the Altyn Tagh fault system in northern Tibet inferred from Cenozoic sedimentation, *Geol. Soc. Am. Bull.*, *114*(10), 1257–1295, doi:10.1130/0016-7606(2002)114<1257:THOTAT>2.0.CO;2.

Zheng, J., X. He, and S. Liu (1999), *Dictionary of Chinese Stratigraphy-Tertiary*, Geology Press, Beijing.

Zhong, S. (1992), Calcareous nannofossils from the Upper Cretaceous and Lower Tertiary in the western Tarim Basin, south Xinjiang, China, *Xinjiang Stratigraphic Res. Ser.*, *5*, 1–121.